MODEL DIESEL BASED INJECTION PROFILE OPTIMIZATION TO REDUCE TRANSIENT SOOT PROFILE

Y C SEKHAR YADAV[1], L SUNIL[2], S PAVAN KALYAN[3]

[123] Department of Mechanical , St.Martin's Engineering College,india.

Abstract: To meet current legislation limits, modern Diesel engines achieve low raw emission levels and utilize complex aftertreatment systems. Still, during fast transients undesired emission peaks may occur for both soot and NOx. These are caused by deviations in the in-cylinder conditions between the quasi steady engine calibration and the transient operation, e.g. during tip-ins. In this work a case study is performed to analyze the potential reduction of transient soot emissions during a specified engine maneuver. An additional target is to investigate potential benefits of a novel in-situ soot sensor based on the Laser Induced Incandescence (LII) principle which offers a high temporal resolution. Measurement data from a Diesel engine is used to develop time varying setpoint deviation models which will be utilized in a numerical optimization problem to determine an optimized injection profile. The modeling and optimization is carried out in parallel for both sensors and results are compared against each other. In the experimental validation the optimized injection profiles were capable of reducing undesired overshoots during transients with minimal impact on the torque response. Furthermore, the novel sensor allows to gain additional insights in the relation between input parameters and soot response, which is reflected by the obtained models and control action.

Keywords: Combustion Control, Compression Ignition, Engine Control

1. INTRODUCTION

Optimizing the transient emission behavior of Diesel engines has been a strong research topic for many years, see e.g Johnson (2016); Rakopoulos et al. (2009); Hagena et al. (2011). Current production level control strategies achieve already very good results. Nonetheless, there is a need for further improvements and alternative strategies. Both, soot and NOx emissions during fast transients present a challenge to the engine control and aftertreatment systems. While fast transient torque changes are desirable from a driver perspective, the limited dynamics of the air system and couplings between fueling and air system can lead to large overshoots in the emission response, see e.g. Alberer and del Re (2009); Selmanaj et al. (2014); Großbichler et al. (2017). Often the target is to reduce these undesired overshoots and achieve a slower first order type response. In industrial approaches for example smoke limiting functions, based on a lambda measurement, or transient reference filters are introduced which adjust the fueling profile to the transient condition of the air system. In academia, many works can be found investigating optimization methods to improve the transient behavior of Diesel engines. A common target is to track NOx, soot and torque trajectories to their stationary setpoints in an optimal way, e.g. in Alberer and del Re (2009) where a model free numerical iterative optimization procedure was

implemented on a testbench to optimize a certain maneuver or in Sequenz et al. (2011) where the authors utilized a dynamical model in a simulation study to optimize airpath actuator trajectories. In Benz et al. (2011) a dynamic simulation environment is applied to optimize actuator trajectories by minimization of integrated emissions. A torque constraint by an inherent torque controller was introduced in the model, to allow a comparison between the different settings. The authors combined airpath and fuel path actuators and evaluated their potential to re- duce the emissions, while keeping the torque response unchanged. Unfortunately, no experimental validation was presented. A similar approach, but with a different objective was considered in Mancini et al. (2014). There for a given fuel trajectory the efficiency was maximized, while an isoperimetric constraint on emissions was considered. These results where implemented as a feedforward strategy on an ECU.

In this work we want to follow and extend above mentioned works with the target of improving the transient soot response of a Diesel engine during a fast operating point change. Moreover, the potential benefits of a novel prototype soot sensor used during the modeling and validation process should be investigated. The idea is to establish static setpoint deviation models (SPD), as in Mancini et al. (2014), for an operating point change scenario and to apply

those models for numerical optimization of selected injection parameter trajectories. To evaluate potential benefits of the novel LII based sensor, all tasks, such as modeling and optimization, are performed in parallel, once with the novel sensor, once using a production standard fast measurement device, namely an Opacimeter. The results are then compared against each other.

For both approaches, the focus is on the offline optimization of a single scenario, to evaluate the soot reduction potential during this transient. The scenario is defined by a load step at constant speed and the optimization is formulated to keep the drivers demand (torque de- mand) unchanged. The optimization acts solely on the fuel path by using the injection parameters $\mathbf{u} = [\Phi_{\text{MI}}, p_{\text{rail}}]^{\text{T}}$. These input variables were chosen, because they show a significant influence on transient emissions, as was ana- lyzed in Selmanaj et al. (2014) and subsequent works e.g. Großbichler et al. (2017) and similar result can be found in Benz et al. (2011). Obviously, injected fuel amount will have an even more significant influence on soot, but also on torque and would be similar to a smoke limit function approach with strong impact on the torque.

The proposed method cannot be implemented in real-time, but allows to evaluate the potential of emission reduction, by optimizing a small set of input parameters. It can be further seen as an important step to determine promising candidates for future research in optimal transient Diesel emission control.

The rest of this work is structured as follows: First the experimental setup is presented. Afterwards, the problem is stated in detail and the modeling procedure is explained. The formulation of the optimization problem and the resulting optimized actuator trajectories are presented. Finally an experimental validation is carried out and a conclusion is given.

2. EXPERIMENTAL SETUP

All measurements to obtain data for modeling and optimization are carried out on a dynamical engine testbench at the Johannes Kepler University (JKU) Linz. The considered engine is a 2 liter 4 cylinder Diesel engine equipped with common rail injection system, cooled high pressure exhaust gas recirculation (EGR) and a variable geometry turbine (VGT) with charge air intercooling. The engine hardware is designed to meet EURO 5 legislation but the actual used calibration does not reflect this certification level anymore, see the next chapter. In order to obtain highly repeatable measurements, engine intake air, fuel and test cell itself are conditioned. The engine torque τ is measured directly at shaft connecting to the electric dynamometer. A Cambustion fNOx 400 is used for NOx measurement x_{NO} $[0, 1]$, which is mounted upstream of the turbocharger. $\in$

To determine the transient soot levels, an AVL Opacimeter as production standard device and the novel soot sensor based on the Laser Induced Incandescence (LII) principle are used. Both sensors are installed directly downstream of the turbocharger and used in parallel. The LII sensor operates at a sampling frequency of 50 Hz and provides due to the in-situ mounting outstanding properties compared

to other available devices, such as faster response time and lower delay times. More details on the novel LII sensor, can be found in Zhang et al. (2017, 2014); Zhang (2017); Viskup et al. (2011).

To compare both sensors, the LII sensor is calibrated to match the Opacimeter values in steady state. The soot signals are denoted as x_{opac} and $x_{\text{opac,LII}}$ $[0, 1]$, respectively. All experiments are executed with a dSpace rapid prototyping system to allow open loop control and data acquisition. The engine is equipped with a development ECU and an open bypass system to directly access airpath and injection parameters.

3. PROBLEM STATEMENT

A main focus is to evaluate the potential of the new in-situ LII sensor to improve the highly transient engine operation. In the particular case study the reduction of undesired soot peaks during tip-ins is investigated. To this end, a single transient engine scenario is considered, defined by constant speed $N = 1250$ rpm and a gas pedal step from $\alpha = 20$ % to $\alpha = 30$ % (tip-in). Of course the experiments can be extended to a larger operating range and different scenarios and be used to improve transient engine control.

Current industrial practice is to implement smoke limiting functions inside an ECU acting on fuel injection amount to reduce the overshoot by following a transient minimum lambda reference. Initial experiments showed that in the case of an activated smoke limiter and with production standard calibration the dynamics of the soot emissions are similar for both considered measurement devices. The measured soot response is mainly depending on the control action and can be measured well by both devices. This is related to the already very high level of production type engine control which is designed to meet emission legislation targets. For our study, we intend to overcome these limitations by deactivating accelerator pedal filters and the smoke limiter functions to obtain a very aggressive step response. Measured experiments of the considered scenario are depicted in Fig. 1.

The resulting transient soot overshoot is very high and can be detected by both x_{opac} and $x_{\text{opac,LII}}$. It is noteworthy that this experimental example is not representing a production standard calibration anymore. Although, a 10 % tip in seems to be rather conservative, without the pedal filters and smoke limiter in the chosen operating point it leads already to a strong response in the opacity signal, see Fig. 1. A larger step was deemed infeasible because it would potentially lead to saturated sensor value during the parameter variation. For our modeling approach it is crucial to obtain information from parameter variations which lead to increase and decrease in the opacity signal

A comparison of the two sensor measurements, for one repetition depicted in Fig. 1, is shown in Fig. 2. Notice that the time delays of the sensors are compensated during an offline data analysis, but the LII sensor shows a faster response. Especially in the phase of decreasing opacity level a large difference between Opacimeter and LII sensor appears. This means, that the Opacimeter detects a decreasing soot level with a slower dynamic than
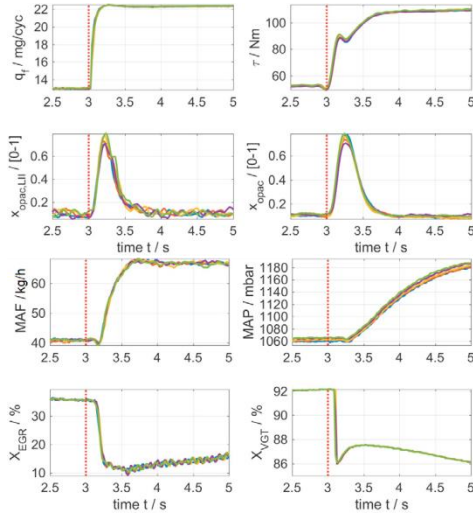
Fig. 1. Considered transient scenario, the experiment was repeated five times to show the reproducibility of the engine behavior

the LII sensor. Based on these observations, the use of the faster LII sensor seems to be beneficial for modeling and lated optimizing the injection profile, because it represents the real soot behavior more accurate and can determine small transient effects which are not detected by standard sensors.
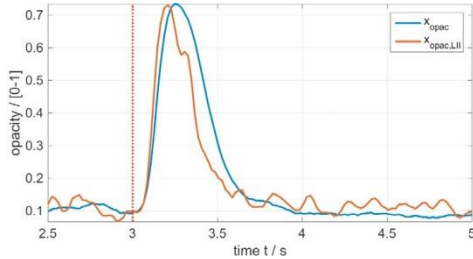

Fig. 2. Comparison of the considered soot sensors during the transient phase of the engine maneuver.

4. MODELING

Modeling Approach

To describe the local behavior of the engine during the transient conditions, a similar approach as in Mancini et al. (2014) is followed, which utilizes static time-varying quadratic setpoint deviation (SPD) models. In our work the considered input variables are $\mathbf{u} = [\Phi_{\mathrm{MI}}, p_{\mathrm{rail}}]^{\mathrm{T}}$ and the outputs are $\mathbf{y} = [x_{\mathrm{opac}}, x_{\mathrm{opac,LII}}, \tau, x_{\mathrm{NO}}]^{\mathrm{T}}$. As one can see, by selecting these inputs $\mathbf{u}$, our approach is different to a standard smoke limiter, which basically changes the main fuel injection amount and therefore affects the torque response. The models are determined for both Opacimeter and LII sensor to be later compared against each other and also to be used in the optimization strategy. A SPD model describes an output deviation $\Delta \mathbf{y}$, resulting from an input deviation $\Delta \mathbf{u}$, relative to a transient reference y_{ref} and u_{ref}, see Fig. 3 for a graphical description of this method. In each sampling time instant, a SPD model is derived from a perturbation of the inputs with respect to the reference (setpoint) trajectory.
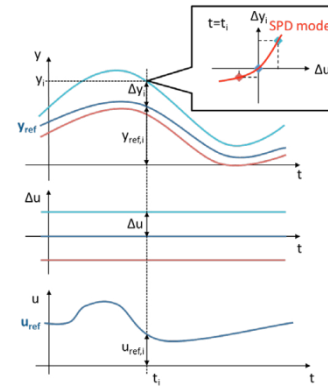

Fig. 3. Illustration of the setpoint deviation model (SPD) identification procedure

Because of the fact, that no airpath actuators are used in this work, no interconnection to the airpath is considered or modeled. This assumption is valid in the case, if the changes in the fuel path are just small and further if the resulting torque is not changed. The latter one means that the exhaust pressure and temperature do not change significantly and therefore no feedback to EGR or turbocharger control arises.

Setpoint Deviation Models

To get reproducible results, the engine should oper- ate in open loop conditions without ECU airpath con- trollers active. For this reason the scenario is mea- sured several times (e.g. five repetitions, as shown in Fig. 1) with standard ECU controllers. By calculat- ing the mean trajectories of these several realizations, a reliable open loop reference of all inputs $\mathbf{U}_{\mathrm{ref}} = [X_{\mathrm{EGR}}, X_{\mathrm{VGT}}, X_{\mathrm{SWR}}, X_{\mathrm{THR}}, q_{\mathrm{MI}}, q_{\mathrm{PI}}, \Phi_{\mathrm{MI}}, t_{\mathrm{PI}}, p_{\mathrm{rail}}]^{\mathrm{T}}$ and con- sidered outputs $\mathbf{y}_{\mathrm{ref}} = [x_{\mathrm{opac}}, x_{\mathrm{opac,LII}}, \tau, x_{\mathrm{NO}}]^{\mathrm{T}}$ can be ob- tained. Using the references $\mathbf{U}_{\mathrm{ref}}$, the engine airpath can be operated in open loop and the reference trajectories for the injection are fixed. The deviation $\Delta \mathbf{u} = [\Delta \Phi_{\mathrm{MI}}, \Delta p_{\mathrm{rail}}]^{\mathrm{T}}$ from the reference inputs $\mathbf{u}_{\mathrm{ref}} \in \mathbf{U}_{\mathrm{ref}}$ is added as a constant perturbation during a scenario to record the output devia- tion $\Delta \mathbf{y} = [\Delta x_{\mathrm{opac}}, \Delta x_{\mathrm{opac,LII}}, \Delta \tau, \Delta x_{\mathrm{NO}}]^{\mathrm{T}}$. The used in- put perturbations are listed in Tab. 1. As one can see, this results in 25 different combinations which have to be mea- sured. Each sequence takes $T = 15$ s and each combination is repeated five times. The sampling frequency is 50 Hz leading to a sampling time $T_s = 20$ ms. The SPD models

Table 1. Perturbation range of the considered input variables

input variable	perturbation values
$\Delta \Phi_{\mathrm{MI}}$	$[-4, -2, 0, 2, 4]$, CAD
Δp_{rail}	$[-100, -50, 0, 50, 100]$ bar

are defined at each time instance $t = kT_s, k = 1, 2, \ldots$ as follows:

$$y_i(t) = y_{\mathrm{ref},i}(t) + \mathbf{g}_i^{\mathrm{T}}(t)\Delta \mathbf{u}(t) + \Delta \mathbf{u}^{\mathrm{T}}(t)\mathbf{H}_i(t)\Delta \mathbf{u}(t) \quad (1)$$

The term $\mathbf{g}_i(t) \in \mathbb{R}^{2\times 1}$ denotes the gradient vector and $\mathbf{H}_i(t) \in \mathbb{R}^{2\times 2}$ the Hessian matrix of the i-th output $y_i(t)$.

$$\mathbf{g}_i(t) = \begin{pmatrix} \theta_{\Phi_{\mathrm{MI}}}(t) \\ \vartheta_{p_{\mathrm{rail}}}(t) \end{pmatrix} ; \mathbf{H}_i(t) = \begin{pmatrix} \theta_{\Phi_{\mathrm{MI}}\Phi_{\mathrm{MI}}} & \frac{1}{2}\theta_{\Phi_{\mathrm{MI}}p_{\mathrm{rail}}} \\ \frac{1}{2}\vartheta_{\Phi_{\mathrm{MI}}p_{\mathrm{rail}}} & \vartheta_{p_{\mathrm{rail}}p_{\mathrm{rail}}} \end{pmatrix} \quad (2)$$

The parameters can be identified at each time instant $t = kT_s$ by applying a Least Squares method. As an example, models obtained for $t = 3.25$ s are depicted in Fig. 4. Although, the variability in the LII signal is higher (blue circles indicating repetitive measurements), the main characteristic are captured and result in a similar shape, like the x_{opac} model. A comparison of the model output trajectories with the measured ones for different input perturbations is shown in Fig. 5. The change of the model
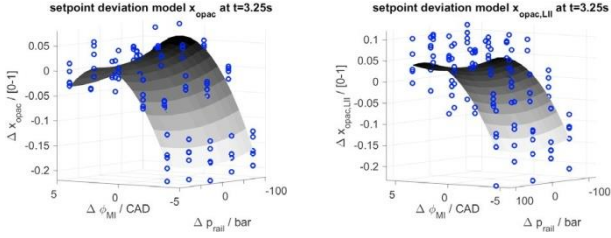parameters over time is depicted in Fig. 6.

Fig. 4. SPD model of x_{opac} and $x_{\mathrm{opac,LII}}$ at $t = 3.25$ s.
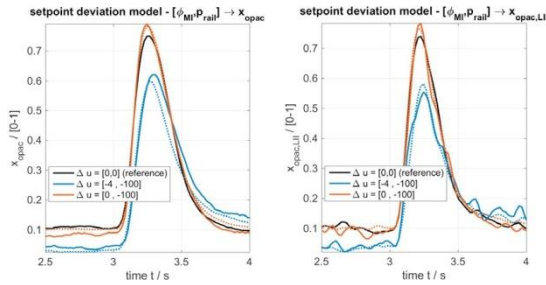

Fig. 5. Comparison of the models. (bold line = measurement, dashed line = model)
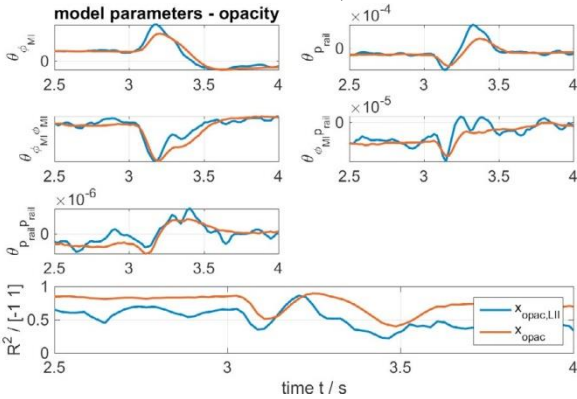

Fig. 6. Model parameters over time for different output variables.

As one can see in Fig. 6, the model parameters change significantly after the step at $T_{\mathrm{step}} = 3$ s occurs. Consequently, this leads to the conclusion, that the local behavior between input and output is changing during the transient phase substantially. In the last subplot the model quality measured by the R^2-value is shown. It should be noted that the low R^2-value for $x_{\mathrm{opac,LII}}$ at the end of the scenario ($t > 3.5$ s) is due to the small deviation of the soot level with respect to the input deviation. In the fast LII

signal the high frequent soot variation dominates in this area, which is not measured by the Opacimeter, see Fig. 5. However, this almost stationary region is not considered in the optimization routine so there is no drawback of using this model.

In Fig. 6 we can observe, that in the stationary condition before and after the maneuver the parameters converge to the same values. Differences between the models mainly occur in the transient phase and especially the influence of p_{rail} should be mentioned. The parameter $\theta_{p_{\mathrm{rail}}}$ changes its sign more quickly in the $x_{\mathrm{opac,LII}}$ model than in the x_{opac} model. The same behavior can be seen in the parameter $\theta_{\Phi_{\mathrm{MI}}p_{\mathrm{rail}}}$. The latter one show an additional change of sign at $t \approx 3.3$ s which cannot be seen in the x_{opac} model at all. These observations are indicating, that the influence of p_{rail} to the soot change faster, than it is possible to capture by the Opacimeter. Thus, an appreciable difference between the resulting optimized injection profiles is expected.

5. OPTIMIZATION

In this section the optimization problem for the transient phase $t \in [3, 4]$ s is formulated.

Optimization Criterion

Focus of this work is the minimization of transient soot peaks while keeping the response to the drivers demand unchanged. The latter one enforces a torque constraint to the optimization process. Many authors in previous works tried to overcome the use of this equality constraint e.g. by using a stationary torque tracking term in the cost function as in Alberer and del Re (2009) or by using an inherent torque feedforward controller in the model like in Benz et al. (2011). In our work we consider this constraint explicitly.

Using the SPD models our intention is to get an optimized injection profile that makes the deviation of soot as negative as possible while keeping the deviation of torque to zero. To analyse the effect of the two different sensors to the optimized injection profile, the two following static optimization problems are formulated

$$
\begin{aligned}
&\min_{\Delta \mathbf{u}} \Delta x_{\mathrm{opac}}(t) && \min_{\Delta \mathbf{u}} \Delta x_{\mathrm{opac,LII}}(t) \\
&\mathrm{s.t.:} \Delta\tau(t) = 0 && \mathrm{s.t.:} \Delta\tau(t) = 0 \\
&t \in [3,4]\,\mathrm{s} && t \in [3,4]\,\mathrm{s} \\
&\Delta \mathbf{u} \in [\Delta\mathbf{u}_{\min}, \Delta\mathbf{u}_{\max}] && \Delta \mathbf{u} \in [\Delta\mathbf{u}_{\min}, \Delta\mathbf{u}_{\max}]
\end{aligned}
\tag{3}
$$

and their results compared against each other in the following. To consider the fact, that the SPD models are just valid in the local region where they were identified, the allowed input deviations are restricted to the range of the identification data, see Tab. 1.

These optimization problems belong to the class of quadratically constraint quadratic programs (QCQP), which can be possibly NP-hard in the nonconvex case (all $\mathbf{H}_i(t)$ are just positive semidefinite).

Optimization Result

In this study, the optimization problem is solved by an interior point algorithm, which is implemented in the Optimization Toolbox for MATLAB.

As a result we obtain for each model optimal input deviation trajectories $\Delta\mathbf{u}_\sigma^* = \arg\{\min_{\Delta\mathbf{u}} \Delta x_\sigma\}$, depending on which model $\sigma = \{\text{opac, opac,LII}\}$ is used in the cost function. The results of the optimization process are shown in Fig. 7.
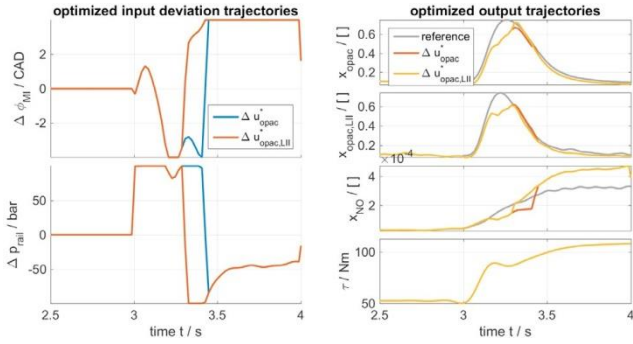

Fig. 7. Resulting optimal deviation trajectories $\Delta\mathbf{u}_\sigma^*(t)$ and model outputs y from the optimization procedure.

The significant difference occurs in the time interval $t \in [3.3, 3.5]$ s, where the inputs change earlier if the model based on the LII sensor is used. This result is consistent with the observations which are made during the iden- tification procedure in the previous section. The torque constraint is fulfilled for both results as one can see in Fig. 7 in the right lower subplot.

The integrated emissions and torque during the time $t \in [3, 4]$ s are calculated and compared to the reference measurement, see Tab. 2. The relative reduction of soot is not that different between the two optimizations and is in the range of about 15 %. Based on this observation, neither Opacimeter nor LII sensor can be identified to provide better results. Additionally, one can see the typical tradeoff with the NOx emissions, which are increased up to 20 % when the soot is reduced and the torque kept constant.

Table 2. Numerical results of the optimization process, the values are normalized relative to the reference trajectory

evaluated value	$\Delta\mathbf{u}_{\text{opac}}^*(t)$	$\Delta\mathbf{u}_{\text{opac,LII}}^*(t)$
$\int_3^4 x_{\text{opac}}(t)dt$	84.3 %	85.7 %
$\int_3^4 x_{\text{opac,LII}}(t)dt$	86.1 %	84.2 %
$\int_3^4 \tau(t)dt$	100.0 %	100.0 %
$10^6 \int_3^4 x_{\text{NO}}(t)dt$	120.9 %	125.5 %

6. EXPERIMENTAL VALIDATION

loop by their reference trajectories $\mathbf{U}_{\text{ref}}(t)$. The validation procedure is carried out as follows: First, the engine is operated using the reference from the identification procedure $\mathbf{U}_{\text{ref}}(t)$. Afterwards, the two optimized inputs $\Delta\mathbf{u}(t)$ are added consecutively. These three scenarios

are repeated several times to limit effects of stochastic variations inherit to the transient combustion process. The mean trajectories of all realizations of each scenario are depicted in Fig. 8.
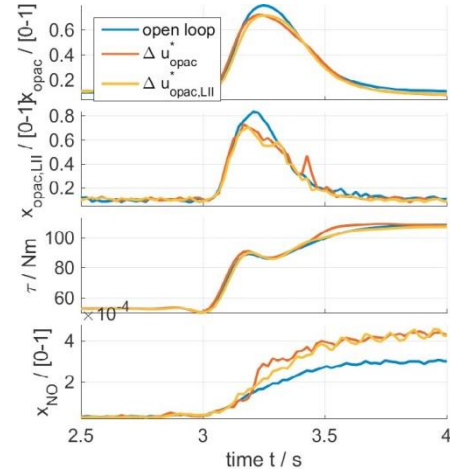

Fig. 8. Output trajectories of the experimental validation.

As can be seen in Fig. 8, the shape of the reduced soot emission is slightly different to those of the simulation, nonetheless, a reduction is possible. Special attention should be denoted to the peak at $t \approx 3.4$ s in the $x_{\text{opac,LII}}$ signal when $\Delta\mathbf{u}_{\text{opac}}^*$ is used. If the input $\Delta\mathbf{u}_{\text{opac,LII}}^*$ is used instead, this peak does not occur anymore. This means, although the fit value of the x_{opac} model seems reasonable, see Fig. 6, the resulting optimized input $\Delta\mathbf{u}_{\text{opac}}^*$ produces an undesired effect which can only be measured by the LII sensor. However, such effect is not observed, when we use $\Delta\mathbf{u}_{\text{opac}}^*$ as input in the model determined from the LII sensor, see Fig. 7. This means, although this effect is reflected by neither the LII nor the Opacimeter based model, by using the LII model a different optimal input trajectory is obtained which does not excite this peak.

The numerical evaluation of integrated emissions and torque is summarized in Tab. 3. As one can see, the relative reduction by using $\Delta\mathbf{u}_{\text{opac,LII}}^*(t)$ is higher than by using the input $\Delta\mathbf{u}_{\text{opac}}^*$. Further, it should be noted, that the torque deviates from its reference trajectory by using $\Delta\mathbf{u}_{\text{opac}}^*$, which leads to an increase of torque of about 2 %. This is maybe one reason why the soot reduction with $\Delta\mathbf{u}_{\text{opac}}^*$ is not that high, but again this shows, that $\Delta\mathbf{u}_{\text{opac,LII}}^*$, based on the LII sensor, is more appropriate to fulfill the optimization targets, i.e. the torque constraint.

Table 3. Numerical results of the validation measurement

evaluated value	$\Delta\mathbf{u}*_{\text{opac}}$	$\Delta\mathbf{u}*_{\text{opac,LII}}$
$\int_3^4 x_{\text{opac}}(t)dt$	94,6 %	91,6 %
$\int_3^4 x_{\text{opac,LII}}(t)dt$	93.7 %	86,9 %
$\int_3^4 \tau(t)dt$	102,0 %	99,6 %
$10^6 \int_3^4 x_{\text{NO}}(t)dt$	141,3 %	136,3 %

To further evaluate the variability of the results, the integrated values of x_{opac} and $x_{\text{opac,LII}}$ for each realization are depicted in Fig. 9. The color indicates the used input and the round markers denote one single realization. The square marker denotes the integral value of the mean

trajectory of all realizations with the corresponding input. As one can see, the realizations using $\Delta \mathbf{u}^*_{\text{opac,LII}}$ lie in the left corner and thus resulting in the largest soot reduction. With $\Delta \mathbf{u}^*_{\text{opac}}$ the achievable reduction is smaller, which is, as mentioned before, partly a result of the deviation from the torque reference. However, it is interesting to see, that the realizations using $\Delta \mathbf{u}^*_{\text{opac}}$ are more widely spread,

compared to those using $\Delta \mathbf{u}^*_{\text{opac,LII}}$. The $\Delta \mathbf{u}^*_{\text{opac,LII}}$ based

ones are well separated from the initial baseline open loop realizations. Thus, in this case a significant reduction of soot emissions is reached with small variations in the single realizations.
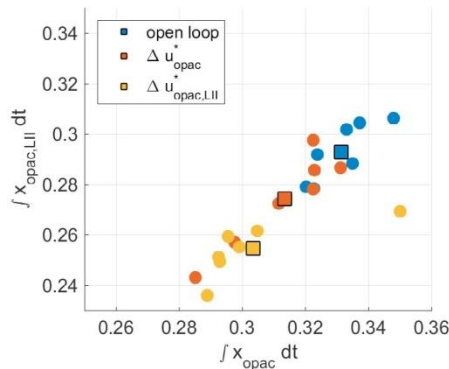

Fig. 9. Comparison of the integrated emissions

7. CONCLUSION

In this work the optimization of the injection profile of a Diesel engine, to minimize soot emissions, is investigated. To estimate the actual soot level, two different sensors, an AVL Opacimeter and a novel sensor based on the Laser Induced Incandescence (LII) principle, are considered. The in-situ LII sensor provides some notable properties compared to other available devices, namely fast measurement dynamics and lower delay time, which benefit the highly transient modeling. The influence of the considered injection parameters to the output variables are modeled by time-varying setpoint deviation models. The use of the models based on the faster LII sensor, allows gaining additional insight into the soot behavior during transients. Especially, the influence of the rail pressure p_{rail} variation could be analyzed more detailed with the LII sensor. The optimized input trajectories are validated by applying them in open loop experiments on a real Diesel engine, showing the potential of reduction of transient soot emissions. Regarding the comparison of both sensors, it can be seen that the application of the optimized trajectory based on the LII sensor model leads to larger reduction of soot.

ACKNOWLEDGEMENTS

REFERENCES

Alberer, D. and del Re, L. (2009). Optimization of the transient Diesel engine operation. Technical report, SAE Technical Paper.

Benz, M., Hehn, M., Onder, C.H., and Guzzella, L. (2011). Model-Based Actuator Trajectories Optimization for a Diesel Engine Using a Direct Method. *Journal of Engineering for Gas Turbines and Power*, 133(3), 032806.

Großbichler, M., Schmied, R., and Waschl, H. (2017). Dynamic Full Range Input Shaping of Injection Param- eters for Reduction of Transient NOx Emissions. *IFAC- PapersOnLine*, 50(1), 3726–3731.

Hagena, J., Assanis, D., and Filipi, Z. (2011). Cycle-resolved measurements of in-cylinder constituents during diesel engine transients and insight into their impact on emissions. *Proceedings of the Institution of Mechanical Engineers, Part D: Journal of Automobile Engineering*, 225(9), 1103–1117.

Johnson, T. (2016). Vehicular Emissions in Review. *SAE International Journal of Engines*, 9(2016-01-0919), 1258–1275.

Mancini, G., Asprion, J., Cavina, N., Onder, C., and Guzzella, L. (2014). Dynamic Feedforward Control of a Diesel Engine Based on Optimal Transient Compen- sation Maps. *Energies*, 7(8), 5400–5424.

Rakopoulos, C., Dimaratos, A., Giakoumis, E., and Rakopoulos, D. (2009). Evaluation of the effect of engine, load and turbocharger parameters on transient emissions of diesel engine. *Energy Conversion and Man- agement*, 50(9), 2381–2393.

Selmanaj, D., Waschl, H., Schinnerl, M., Savaresi, S., and del Re, L. (2014). Dynamic Injection Adaptation by In- put Shaping for Low NOx Emissions during Transients.Technical report, SAE Technical Paper.

Sequenz, H., Mrosek, M., Zydek, S., and Isermann, R. (2011). Model Based Optimisation of a Step in Acceleration for a CR-Diesel Engine. *IFAC Proceedings Volumes*, 44(1), 13016–13021.

Viskup, R., Alberer, D., Oppenauer, K., and del Re, L. (2011). Measurement of transient PM emissions in diesel engine. Technical report, SAE Technical Paper.

Zhang, Z. (2017). *Fast measurement and estimation of transient soot emission from a production Diesel engine*. Ph.D. thesis.

Zhang, Z., del Re, L., and Fuerhapter, R. (2017). Fast Hy- brid Sensor for Soot of Production CI Engines. Technical report, SAE Technical Paper.

Zhang, Z., Stadlbauer, S., Viskup, R., Fuerhapter, R., del Re, L., Bergmann, A., and Reinisch, T. (2014). Fast measurement of soot by in-situ LII on a production engine. In *ASME 2014 Internal Combustion Engine Division Fall Technical Conference*. American Society of Mechanical Engineers.